

A PARAMETRIC INVESTIGATION OF THE TRANSITION BETWEEN BEAM-WEB SHEAR BUCKLING AND BOTTOM-FLANGE BUCKLING AT ELEVATED TEMPERATURES

Guan Quan, Shan-Shan Huang & Ian Burgess, *University of Sheffield, UK*

ABSTRACT

In this research, two existing analytical models of beam-web shear buckling and bottom-flange buckling in steel beams at elevated temperatures have been briefly reviewed. Both models are able to track the behaviour from pre-buckling to post-buckling stage, near to the ends of beams. A transition criterion has been proposed to justify which buckling phenomenon occurs in reality, according to the given structural information, such as geometrical dimensions and loading conditions. A number of 3D finite element models have been created using the ABAQUS software. Parametric studies have been carried out to detect the transition from beam-web shear buckling to bottom-flange buckling, as well as an interactive range within which both phenomena occur simultaneously. Comparisons between the analytical and FE models have shown that it is possible to propose criteria to detect the transition between buckling types. The proposed analytical methods provides sufficient accuracy to be developed further, and in due course it will be embodied in global modelling of composite structures in fire as part of a component-based approach to connections and their adjacent zones.

1. INTRODUCTION

The Cardington fire tests in 1995-96 indicated that both beam-web shear buckling and beam bottom-flange buckling, near to the ends of steel beams, are very prevalent under fire conditions, as shown in Fig. 1. These phenomena can cause significant effects on the adjacent connections, as well as changing the force distribution between different parts of the structure at high temperatures, when performance-based structural fire engineering analysis is carried out. Analytical models [1] have been proposed to track the force-deflection behaviour when pure shear buckling behaviour of the beam web occurs, or beam-web shear buckling and flange buckling occur simultaneously at elevated temperatures. These analytical models will be implemented in the software Vulcan as independent components, based on a component-based method. Therefore, a transition criterion is needed in order to justify whether beam-web shear buckling or bottom-flange buckling will actually occur according to the structural information of a particular case.

2. BEAM-WEB SHEAR BUCKLING AND BOTTOM-FLANGE BUCKLING MODELS

The analytical models which will be reviewed are those for beam-web shear buckling and bottom-flange buckling, proposed by Quan [1, 2]. Both of

these two models are able to predict the buckling behaviour well for Class 1 and Class 2 beams [3] at elevated temperatures, under the assumption that the corresponding buckling mode has already been triggered. The two buckling modes cannot occur simultaneously.



Fig. 1. Shear buckling and bottom-flange buckling in Cardington fire test [4]

2.1 THE ANALYTICAL MODEL OF SHEAR BUCKLING

The shear buckling model is based on the classical tension field theory [5]. This proposed model is able to produce a tri-linear force-displacement relationship for any shear panel, from initial loading to failure. An example characteristic is shown schematically in Fig. 2. The characteristic divides the response into three stages: the elastic, plastic and plastic post-buckling stages. In Fig. 2 Point 1 represents the end of the elastic stage.

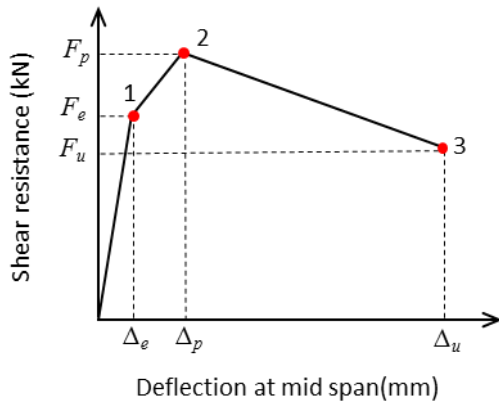


Fig. 2. Schematic tri-linear force–deflection response of a shear panel [1]

In the elastic stage, no buckling occurs in the panel. The beam web is assumed to be composed of tensile and compressive strips. The tensile stresses within the tensile strips are equal to the compressive stresses within the compressive strips. The beam shear resistance and deflection can be calculated according to Eurocode 3 [3] as usual, assuming elastic bending moment and shear force. The elastic stage is shown in Fig. 3 (a).

Point 2 represents the initiation of buckling. The phase between Point 1 and Point 2 is the plastic stage. In this stage, tensile and compressive stresses still remain identical. The von Mises stress lies between the proportional limit stress and the yield stress. Two plastic hinges occur on each of the top and bottom flanges. The model of the elastic stage is shown in Fig. 3 (b).

Point 3, at which the strain is the end of the yield plateau in the high-temperature material stress – strain characteristic according to Eurocode 3 [3], refers to the end of the analysis. The phase between Points 2 and 3 is the plastic post-buckling stage. During this stage, the compressive stresses reduce due to beam-web shear buckling while tensile stresses are enhanced. The part of the web between the four plastic hinges forms a mechanism, enabling transverse drift of the shear panel. The model of the plastic post-buckling stage is shown in Fig. 3 (c).

The calculation principle is based on the equality of the internal work and the loss of potential energy of the external shear force.

$$W_{int} = W_{ext} \quad (1)$$

Following this calculation, the distance between plastic hinges which satisfies this criterion with the lowest internal work can be calculated.

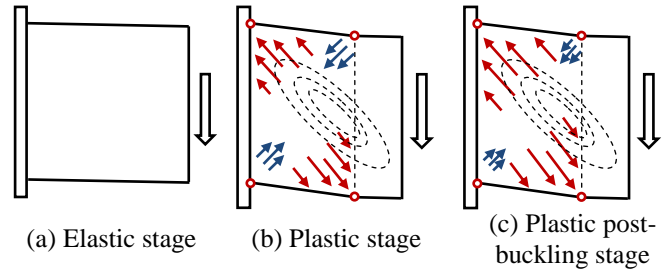


Fig. 3. Shear buckling behaviour at different stages [1]

2.2 THE ANALYTICAL MODEL OF BOTTOM-FLANGE BUCKLING

The analytical model is based on Dharma's model [6] for steel beams at elevated temperatures. This adopts the yield-line mechanism shown in Fig. 4.

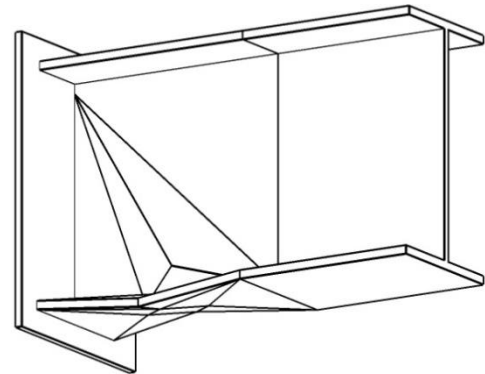


Fig. 4. Yield line mechanism of bottom-flange buckling

This divides the loading procedure into three stages: pre-buckling, plateau and post-buckling, as shown in Fig. 5.

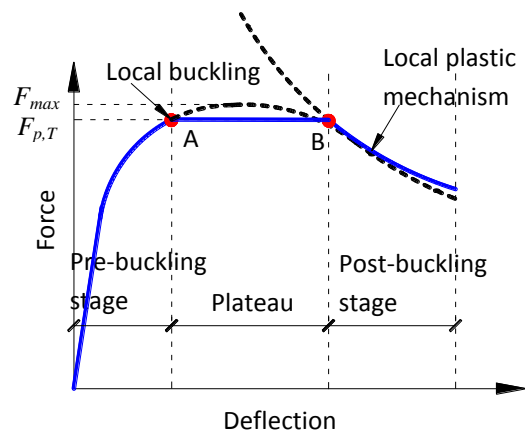


Fig. 5. Schematic force–deflection curve of a buckling panel

The pre-buckling stage follows the normal calculation rules for beams at elevated temperatures. The plateau AB occurs at the reaction force when the sectional plastic moment

capacity is reached at the middle of the buckling zone. The Point B is the point at which bottom-flange buckling occurs. It is assumed that the collapse mechanism is composed of both yield lines and plastic axial-yield zones.

When the flange rotates, compatibility exists between the flange and its connected beam web, assuming that the flange and the adjacent web always remain perpendicular to each other. Therefore, pure flange buckling never occurs. The beam web will always buckle in order to be compatible with the flange buckling. However, in order to distinguish beam-web shear buckling and the combination of flange buckling and beam-web buckling, the latter buckling mode is only called bottom-flange buckling in this research.

It has been proved, on the basis of a number of investigations [1] that the real structural resistance is very close to the plastic shear capacity when plastic shear buckling occurs for Class 1 or Class 2 beams. The bottom-flange buckling theory is consistent with the real structural resistance when bottom-flange buckling occurs. Therefore, either shear buckling or bottom-flange buckling can happen, depending on whether the plastic shear resistance or the plastic moment capacity occurs first. The calculation procedure to detect the transition from beam-web shear buckling to bottom-flange buckling is shown in Fig. 6. It is worth noting that in this flowchart the plastic moment capacity M_p considers the effect of shear

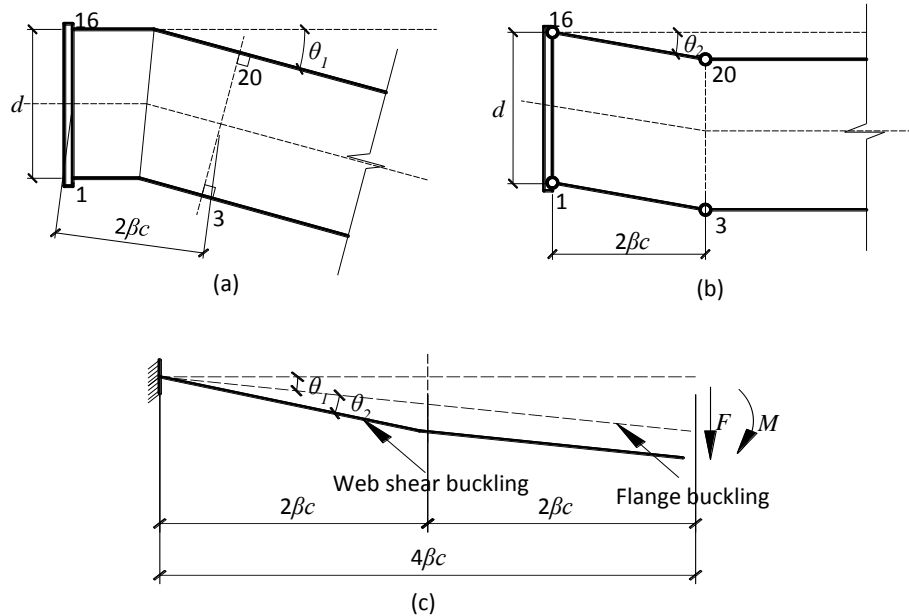


Fig. 1. The effects of flange buckling and beam-web shear buckling on beam vertical deflection (a) Deflection caused by flange buckling; (b) Deflection caused by shear buckling; (c) Deflection of the whole

The effects of these two buckling phenomena are considered separately. The deflection of the buckling zone is composed of the total deflection caused by both bottom-flange buckling and beam-web shear buckling, as shown in Fig. 5 (c). The effect of bottom-flange buckling is to cause a rotation of the whole beam-end about the top corner of the beam, as shown in Fig. 5 (a). The influence of shear buckling is a transverse drift of the shear panel, as shown in Fig. 5 (b).

3. CALCULATION PROCEDURE TO DETECT THE TRANSITION CRITERIA

force on this moment resistance if the shear force is more than half of the plastic shear resistance, which is the rule according to Eurocode 3 [7]. The calculation principle is also based on Eq. (1).

4. VALIDATION AGAINST ABAQUS MODELS

The commercial finite element software ABAQUS has been used to simulate the buckling phenomena in the vicinity of beam-column connections at 415 °C. The four-noded shell element S4R [8], which is capable of simulating buckling behaviour, was adopted. A mesh sensitivity analysis was carried out. A 15mm x 15mm element size, which

achieves optimum accuracy and efficiency, has been used after the mesh sensitivity analysis. The Riks approach was used in order to identify the descending part of the force-displacement curve after inelastic buckling occurs.

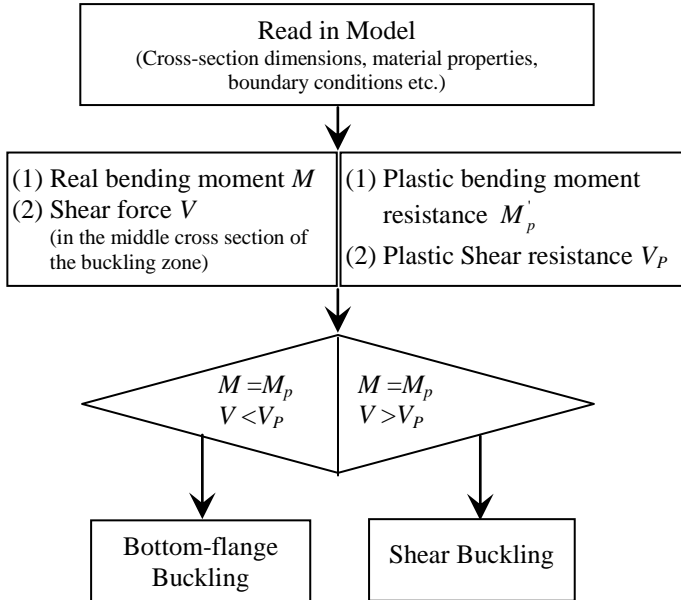


Fig. 6. Flowchart of calculation procedure to determine buckling type.

4.1 DEVELOPMENT OF THE ABAQUS MODELS

Two groups of ABAQUS models with the same cross-section dimensions were developed in order to validate the beam-web shear buckling model and bottom flange buckling model, as well as the criteria for the transition between these two buckling types. The cross-section dimensions used are shown in Fig. 7.

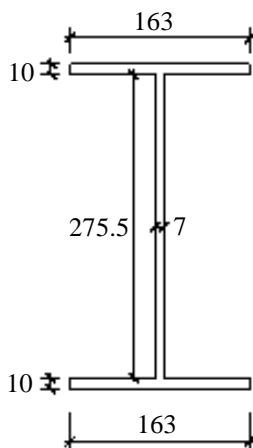


Fig. 7. Cross-section dimensions of the ABAQUS models (mm)

For the first set of analyses (Group A), cantilever beams with lengths from 750mm to 2000mm were analysed. In Group B, fully restrained beams with lengths from 2000mm to 6000mm were analysed. Only the part from one end to the point of inflection was modelled, in order to avoid an undue influence from bending moment-induced curvature. Uniformly distributed load was applied to both groups. For Group B, an additional shear force, representing that transferred from the other connected part of the beam, was applied to the end of the ABAQUS model. The ABAQUS meshing, as well as the loading and boundary conditions for Groups A and B are shown in Fig. 8.

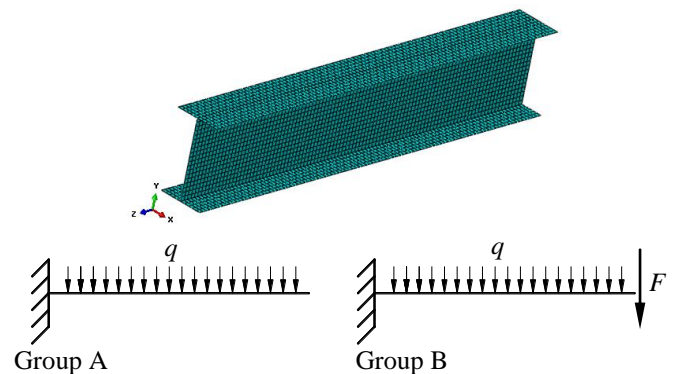


Fig. 8. ABAQUS image, loading conditions and boundary conditions

The ABAQUS models were first uniformly heated to 415 °C, and then load was applied to the beams until buckling occurred. A static-Riks approach was carried out in the post-buckling stage to track the descending force-deflection relationship. The stress-strain relationship of the beam material at 415 °C was defined according to Eurocode 3 [3]. The details of the material properties used in the ABAQUS models are shown in Table 1.

Table 1. Material Properties

$f_{y,\theta}$ (N/mm ²)	$\varepsilon_{y,\theta}$ (%)	$\varepsilon_{t,\theta}$ (%)	$\varepsilon_{u,\theta}$ (%)	$E_{\alpha,\theta}$ (N/mm ²)
267.96	2	15	20	1.411×10^5

Strain hardening of steel is negligible at high temperatures. The constitutive model for structural steel at elevated temperatures is shown in Fig. 9.

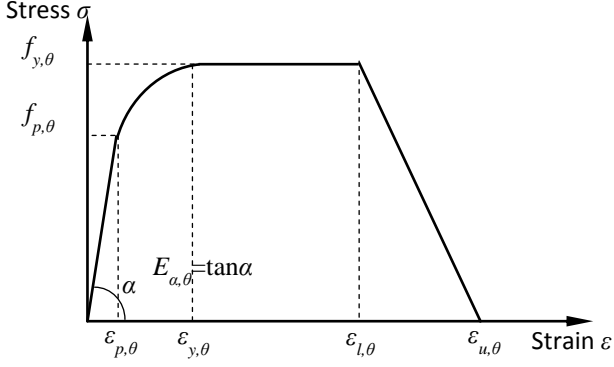


Fig. 9. Constitutive stress-strain relationship for structural steel at 415°C

4.2 COMPARISON WITH THE ANALYTICAL MODEL

Comparisons were made between ABAQUS simulations and the beam-web shear buckling and bottom-flange buckling analytical models for Groups A and B, which were introduced in Section 4.1. The results for Group A are shown in Fig. A 1. Four lengths from 750mm to 2000mm with the same cross-section dimensions were analysed as cantilevers. The square-marked line, which is denoted “Elastic-plastic”, represents the force-deflection relationship when the plastic moment resistance is reached at the middle of the flange buckling zone. The length of the buckling zone is always considered to be identical to the beam depth, as this assumption simplifies the calculation without being a major influence on the accuracy. The smooth line without markers represents the result of finite element modelling. The lines with circular markers and triangular markers are the results from the pure shear and bottom-flange buckling theories respectively. The finite element result can be regarded as accurate. It can be seen that, for the 750mm beam, the shear buckling curve compares well with the FEA result. These are both below the Elastic-plastic curve. The bottom-flange buckling result is considerably above the FEA modelling. This indicates that beam-web shear buckling is the actual buckling mode. As the cantilever length reaches 1000mm, both the shear buckling result and the FEA result begin to approach the Elastic-plastic curve, as does the bottom-flange buckling analysis. This is the transition phase within which the buckling mode changes from beam-web shear buckling to bottom-flange buckling. For cantilevers with lengths of 1500mm and 2000mm, both the FE

results and bottom-flange buckling theoretical results remain in the vicinity of the Elastic-plastic curve. The two results compare well, while the shear buckling analytical result starts to rise above the FEA and bottom-flange buckling curves. This indicates that bottom-flange buckling is the preferred buckling mode for the 1500mm and 2000mm cantilevers. For this cantilever cross-section dimensions, the transition length should be around 1000mm according to these results. This conclusion is also indicated by the ABAQUS result visualizations shown in Fig. 10.

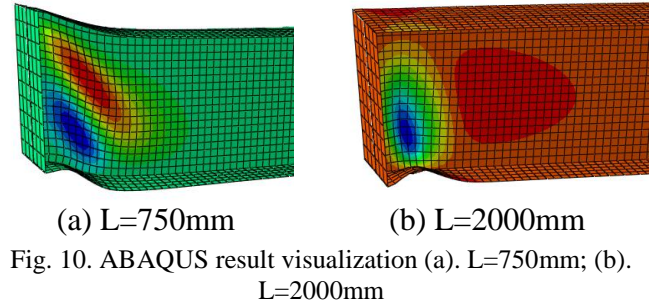


Fig. 10. ABAQUS result visualization (a). L=750mm; (b). L=2000mm

It is worth noting that the analytical results for bottom-flange buckling start to be consistent to the FEA when the finite element results approach the Elastic-plastic curve. This indicates that it is reasonable to regard the beam plastic bending moment capacity as one of the determinants of the transition.

According to the calculation procedure in Section 3, the plastic shear resistance is given as:

$$V_p = \frac{A_v (f_{y,\theta} / \sqrt{3})}{\gamma_{M0}} \quad (2)$$

where A_v is the shear area.

The plastic moment capacity considering the effect of coexisting shear force is:

$$M'_p = (1 - \rho) M_p \quad (3)$$

Where M_p is the fully plastic moment capacity of the cross section. ρ can be expressed, according to Eurocode 3 [9], as:

$$\rho = \left[\frac{2V_{Ed}}{V_p} - 1 \right]^2 \quad (4)$$

Where V_{Ed} is the elastic shear resistance of the cross-section. The calculated transition length from this procedure is 1036mm. This is consistent with that derived not only from the FE analysis visualization, but also from the comparison between the analytical models and the FE analysis.

Another group (Group B) of fully-restrained beam examples were analysed. The results are shown in Fig. A 2. The Group B results were inspected in similar fashion to Group A. It can be seen that the transition length for this group is around 3000mm. Two ABAQUS result visualizations are shown in Fig. 11.

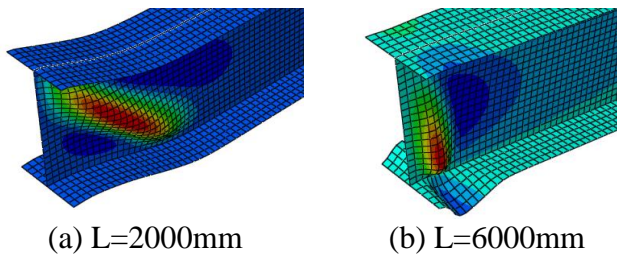


Fig. 11. ABAQUS result visualization (a). $L=2000\text{mm}$; (b). $L=6000\text{mm}$

The transition length calculated from the procedure given in Section 3 is 3195mm, which again compares well with the FE analysis and the analytical models. According to the two groups of examples analysed, it can be suggested that the proposed transition criterion is an easy and effective way of identifying the lengths of beams at which the local buckling type changes.

5. CONCLUSIONS

A brief review of two analytical models of beam-web shear buckling and bottom-flange buckling has been presented. The primary goal was to create a simple criterion and the corresponding calculation procedure to detect the transition between buckling types.

REFERENCES

1. G. QUAN, S.-S. HUANG, and I. BURGESS, 2015 'An analytical approach to modelling shear panels in steel beams at elevated temperatures', *Engineering Structures*, vol. 85, pp. 73-82.
2. G. QUAN, S.-S. HUANG, and I. BURGESS, 2015 'Component-based model of steel-beam buckling panels at elevated temperatures (manuscript)'.
3. CEN, 2005 'BS EN 1993-1-2. Design of steel structures. Part 1.2: General rules - Structural fire design', ed. UK: British Standards Institution.
4. G. NEWMAN, J. T. ROBINSON, and C. G. BAILEY, 2001 'Fire safe design: A new approach to multi-storey steel-framed buildings', *SCI publication*, vol. 288.
5. K. ROKEY and M. SKALOUD, 1927 'The ultimate load behaviour of plate girders loaded in shear', *The Structural Engineer*, vol. 50, pp. 29-48.
6. R. B. DHARMA, 2007 'Buckling behaviour of steel and composite beams at elevated temperatures'. Ph.D. thesis. Nanyang Technological University; 2006.
7. CEN, 2006 'BS EN 1993-1-5. Eurocode 3. Design of steel structures. Part 1.5: Plated structural elements', ed. UK: British Standards Institution.

Two groups of beams were analysed using the finite element software ABAQUS and the existing analytical models for beam-web shear buckling and bottom-flange buckling. It was observed from comparison of the results that, when beam length is shorter than the transition length, shear buckling is the dominant buckling mode. The shear buckling curve from the analytical model fits the FE results well. The bottom-flange buckling analytical results lie above the shear buckling curve and the FE results, indicating that bottom-flange buckling cannot occur. When the beam length is longer than the transition length, bottom-flange buckling is the dominant buckling mode. The analytical results for bottom-flange buckling compare well with the FE analysis. The shear buckling analytical result then lies above the other two curves. For the beams with lengths around the transition length, the FEA, shear buckling and bottom-flange buckling results tend to be almost identical. The transition lengths observed from the FE modelling and the comparison between the analytical and FE models are consistent with the transition lengths according to the calculation process shown in Fig. 6 for the two groups of beams analysed. Although a more extensive parametric validation is needed; the effects of the compressive force caused by thermal restraint or by the restraint of concrete slab in composite structures, as well as the effects of tensile force in the catenary stage, need to be considered in the future, this process seems a simplified and effective way to detect the beam lengths at which the transition occurs between beam-web shear buckling and bottom-flange buckling.

8. D. HIBBIT, B. KARLSSON, and P. SORENSON, 2005 'ABAQUS reference manual 6.7', ed: Pawtucket: ABAQUS Inc.
9. CEN, 2005 'BS EN 1993-1-1. Design of steel structures. Part 1.1: General structural rules', ed. UK: British Standards Institution.

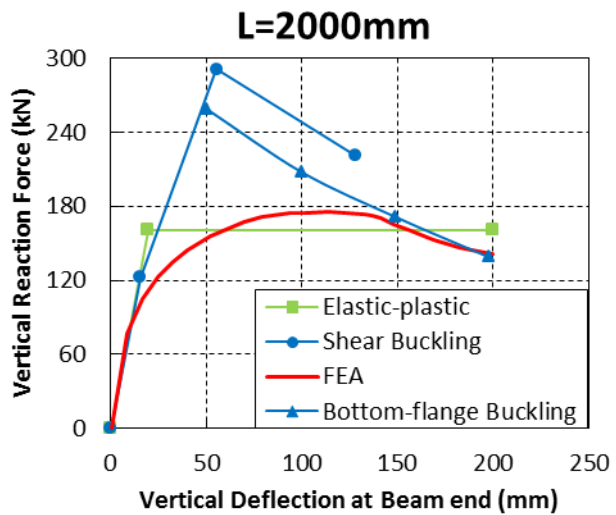
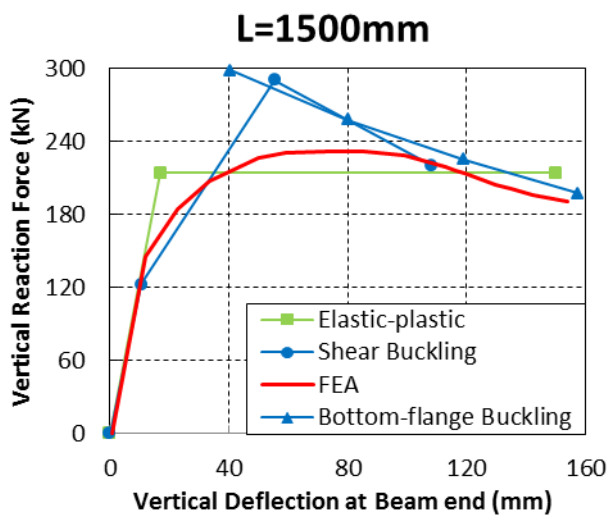
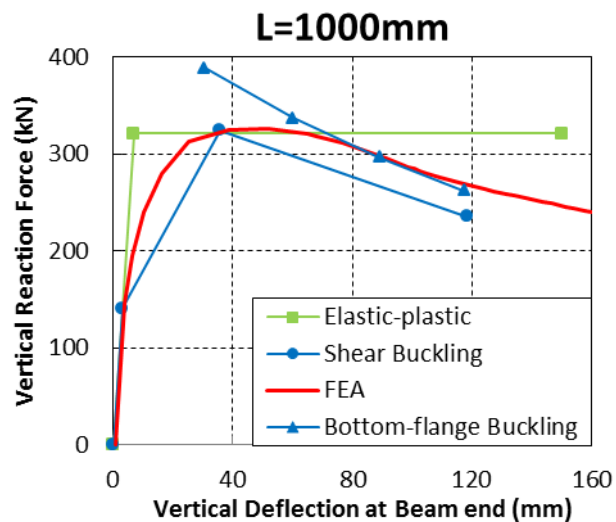
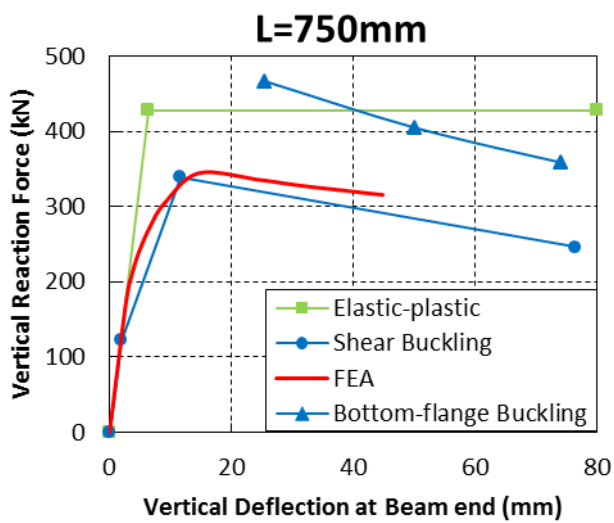


Fig. A 1 Comparison between the analytical and FE models for Group A

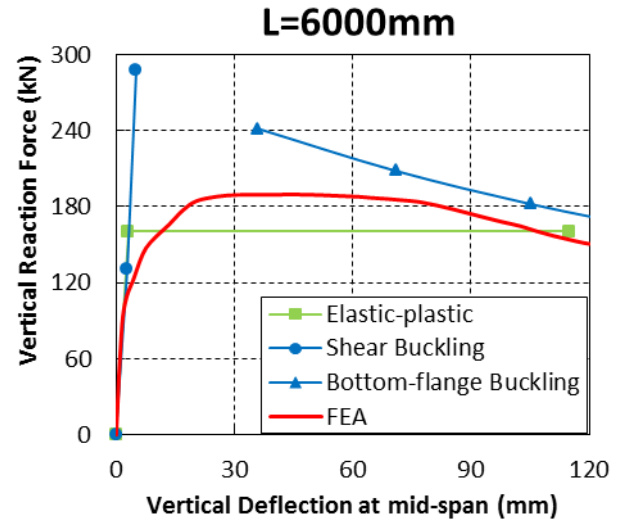
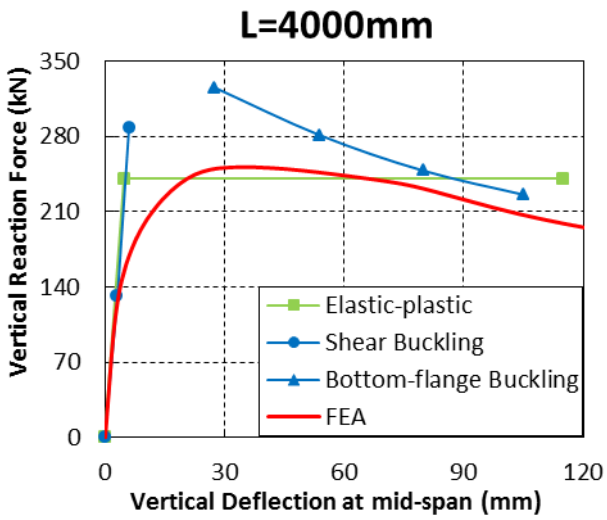
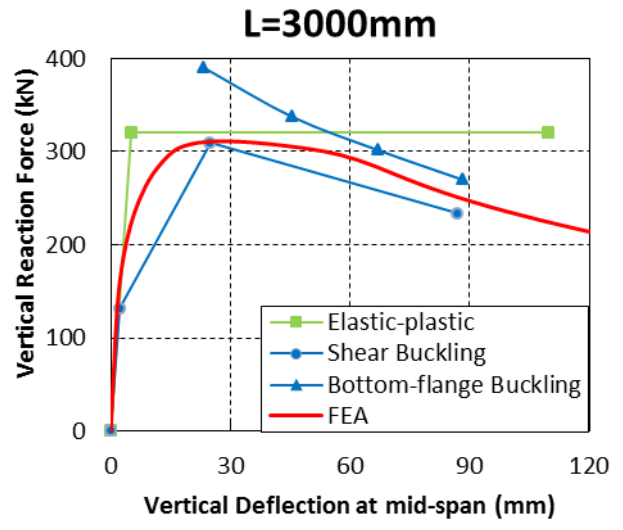
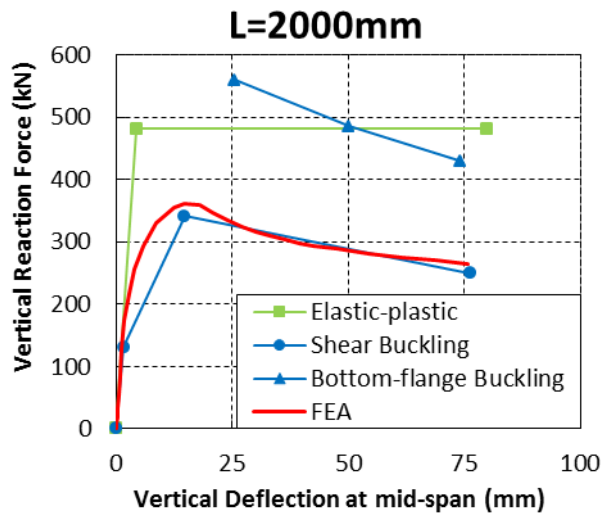


Fig. A 2 Comparison between the analytical and FE models for Group B